Experimental State Tomography of Itinerant Single Microwave Photons

C. Eichler, D. Bozyigit, C. Lang, L. Steffen, J. Fink, and A. Wallraff

Department of Physics, ETH Zürich, CH-8093, Zürich, Switzerland

(Received 8 December 2010; published 1 June 2011; corrected 3 June 2011)

A wide range of experiments studying microwave photons localized in superconducting cavities have made important contributions to our understanding of the quantum properties of radiation. Propagating microwave photons, however, have so far been studied much less intensely. Here we present measurements in which we reconstruct the quantum state of itinerant single photon Fock states and their superposition with the vacuum by analyzing moments of the measured amplitude distribution up to fourth order. Using linear amplifiers and quadrature amplitude detectors, we have developed efficient methods to separate the detected single photon signal from the noise added by the amplifier. From our measurement data we have also reconstructed the corresponding Wigner function.

DOI: 10.1103/PhysRevLett.106.220503 PACS numbers: 03.67.Bg, 42.50.Dv, 42.50.Lc, 42.50.Pq

The quantum properties of microwave frequency photons localized in space are typically investigated in the context of cavity quantum electrodynamics (QED) experiments with Rydberg atoms [1,2] or superconducting circuits [3–5]. Propagating (itinerant) individual microwave photons have been generated [6], but their quantum properties have not yet been studied with the same intensity. This is partly due to the fact that efficient single photon counters in this frequency domain are still under development [7]. However, recently it was shown that characteristic quantum properties of propagating microwave photons, such as antibunching, can be observed in correlation measurements using linear amplifiers and quadrature amplitude detectors [8,9]. In the context of circuit QED [3,4], propagating microwaves are also used to control [10] and readout the quantum state of artificial atoms [11] and to observe phenomena such as resonance fluorescence [12].

In general, the quantum state of any field mode a is characterized by its density matrix ρ or an equivalent quasiprobability distribution such as the Wigner, the Husimi Q, or the Glauber-Sudarshan P function [13,14]. Less widely appreciated, the mode a is also equivalently specified by the infinite set of its moments $\langle (a^\dagger)^n a^m \rangle$ [15]. In this work we use measurements of such field moments up to fourth order to characterize single photon states.

In the optical domain many experimental techniques exist to reconstruct the quantum state of light using square law detectors [16]. In most instances, homodyne detection schemes are used to record the statistical properties of single quadrature components for different local oscillator phases, known as optical tomograms, which allow for a reconstruction of the Wigner function by an inverse Radon transformation [17]. Alternatively, in heterodyne detection schemes the joint statistics of two conjugate quadrature components, described by the Husimi Q distribution, are measured [18]. Both techniques allow for the full reconstruction of the quantum state of a single field mode.

In the microwave domain linear amplifiers are used to measure the amplitude of the signal instead of its intensity. In this case, one can realize a homodyne detection scheme using phase sensitive amplifiers. They ideally amplify only one quadrature of the signal noiselessly while deamplifying the other quadrature. However, state-of-the-art conventional linear amplifiers are phase insensitive, amplifying both quadratures of the signal equally while adding at least the vacuum noise to the signal but usually much more. Using these amplifiers heterodyne detection is realized in our experiments, where conjugate quadratures are measured simultaneously for a fixed local oscillator phase [19,20].

Here we demonstrate photon state tomography using such phase insensitive amplifiers in combination with heterodyne detection of both field quadratures. We first discuss the relation between the single propagating field mode and the resonator mode acting as the photon source (see Fig. 1). Then we describe a method to systematically separate the signal from the noise using a single linear amplifier chain. Similar methods have recently been discussed for a setup with two linear amplifier channels [21]. Finally, we use this method to reconstruct the Wigner function of a single photon Fock state and its superposition with the vacuum state.

We realize a single photon source in a circuit QED setup employing a transmission line resonator of frequency $\nu_r \approx 6.77$ GHz coupled to a single transmon qubit with vacuum Rabi rate $2g/2\pi \approx 146$ MHz [9]. By tuning the qubit prepared in a superposition state $\alpha|g\rangle + \beta|e\rangle$ into the resonator for exactly half a vacuum Rabi period, we generate a single photon state $\alpha|0\rangle + \beta|1\rangle$ [9,22]. The state preparation time is short compared to the cavity decay time $\tau = 1/\kappa \approx 40$ ns. We repeat the photon generation every 800 ns, which allows us to prepare approximately 4×10^9 single photon states per hour.

The field generated in the resonator then decays into the output mode a_{out} related to the resonator mode A by the

input-output boundary condition $a_{\text{out}}(t) = \sqrt{\kappa}A(t) - a_{\text{in}}(t)$ [23], where a_{in} is in the vacuum state; see Fig. 1. We integrate the output signal over a weighted time window $f(t)$ to define a single time independent mode $a = \int dt f(t) a_{\text{out}}(t)$. Considering the resonator dynamics $A(t) = e^{-\kappa t/2}A(0) + \sqrt{\kappa}e^{-\kappa t/2}\int_0^t d\tau e^{\kappa\tau/2}a_{\text{in}}(\tau)$ [24], the choice $f(t) = \sqrt{\kappa}e^{-\kappa\tau/2}\Theta(t)$, where $\Theta(t)$ is the Heaviside step function, leads to the identity $a = A(0)$. Therefore, a is in the same quantum state as the resonator at the preparation time $t = 0$.

To characterize the state of mode a we first pass the signal through a phase insensitive amplifier chain with effective gain G, which introduces an additional noise mode h. The amplified signal is then split into two equal parts and mixed with an in-phase and out-of-phase local oscillator, respectively, to simultaneously detect the conjugate quadrature components $\hat{X}$ and $\hat{P}$. Consequently, $\hat{X}$ and $\hat{P}$ are related to a and h by

$$\sqrt{G}(\hat{X} + i\hat{P}) = \sqrt{G}(a + h^\dagger) \equiv \hat{S} \tag{1}$$

defining the complex amplitude operator $\hat{S}$ [8].

If the amplifier is quantum limited, i.e., the noise mode h is in the vacuum state, it has been shown that the quantum state at the amplifier output can be expressed in terms of the Husimi Q function $Q_{\text{out}}(\sqrt{G}\alpha) = Q_{\text{in}}(\alpha)/G$ [25]. This implies that the Q function remains invariant under the amplification process up to a scaling factor. Therefore the measurement results of the operator $\hat{S}$ are distributed as $Q_{\text{out}}(S)$.

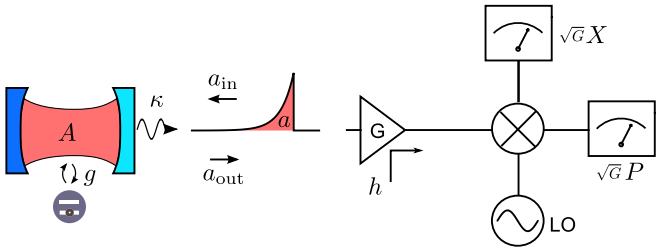

FIG. 1 (color online). Simplified schematic of the experimental setup. An optical analog of the photon source realized in our experiments is shown as a single sided cavity with one highly reflective and one partially transmitting mirror. A single photon is generated in the cavity by preparing the qubit in its excited state when detuned from the cavity and then tuning it into resonance with the cavity for half a vacuum Rabi period $\pi/2g$. The photon is then emitted at a rate κ into the output mode a_{out} resulting in an exponentially decaying envelope of the single photon pulse while the mode a_{in} remains in the vacuum state. The signal is then amplified with effective gain G and noise in mode h is added [8,19]. The amplified signal is down-converted in a microwave quadrature mixer using a local oscillator (LO). The two quadrature amplitudes X and P are recorded using an analog-to-digital converter and stored in real time in a two-dimensional histogram using field programmable gate array electronics. An optical frequency analog of our measurement scheme is discussed in detail in [8].

The best commercially available amplifiers for frequencies below 10 GHz add thermal noise with an effective temperature of $T_{\text{noise}} \approx 2$ K and therefore are far from being quantum limited. Typically, the noise mode h is then in good approximation in a thermal state represented by a Gaussian phase space distribution. As shown in Ref. [26], the measured distribution of $\hat{S}$ at the amplifier output

$$D^{[\rho]}(S) = \frac{1}{G}\int d^2\beta P_a(\beta) Q_h(S^*/\sqrt{G} - \beta^*) \tag{2}$$

can then be interpreted as the convolution of the P function of mode a and the Q function of the noise mode h.

We store the results of repeated measurements of $\hat{S}$ (i.e., the instantaneous values of X and P) in a two-dimensional histogram with 1024×1024 entries, which corresponds to a discretized version of the probability distribution $D^{[\rho]}(S)$. To extract the properties of mode a alone we perform two measurements. One in which mode a is left in the vacuum serving as a reference measurement for the noise, where $P_a(\beta) = \delta^{(2)}(\beta)$ is a two-dimensional Dirac δ function [14], resulting in the distribution

$$D^{[|0\rangle\langle 0|]}(S) = \frac{1}{G}Q_h(S^*/\sqrt{G}), \tag{3}$$

and a second one in which the state of interest $|\psi\rangle$, such as a Fock state $|1\rangle$, is prepared. In practice both histograms are accumulated in an interleaved fashion, changing between the two cases every 25 μs to avoid systematic errors due to drifts. The measured histograms for both vacuum $D^{[|0\rangle\langle 0|]}$ and for a Fock state $D^{[|1\rangle\langle 1|]}$ are dominated by the noise added by the amplifier; see Figs. 2(a) and 2(b). However, when calculating the numerical difference of

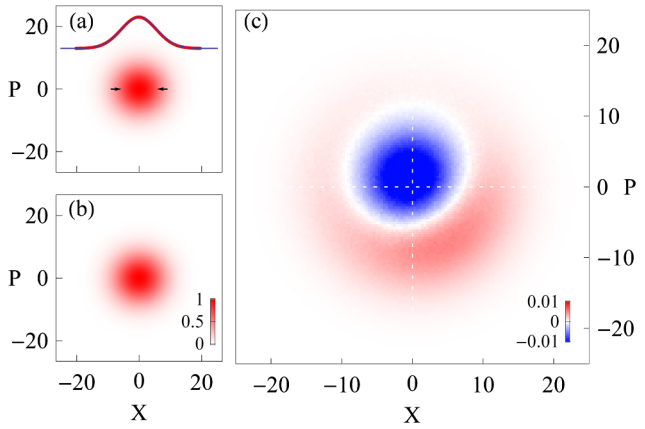

FIG. 2 (color online). (a) Measured quadrature histogram $D^{[|0\rangle\langle 0|]}(S)$ for a in the vacuum where $S = \sqrt{G}(X + iP)$. The inset shows a horizontal cut through the histogram (thick red curve). The distribution is well described by a normal distribution (thin blue curve) with width $\sigma = 5.7$ (indicated by black arrows) corresponding to a system noise temperature of $T_{\text{noise}} \approx 21$ K. (b) Quadrature histogram $D^{[|1\rangle\langle 1|]}(S)$ for preparation of single photon Fock states. (c) Difference of $D^{[|1\rangle\langle 1|]}(S)$ and $D^{[|0\rangle\langle 0|]}(S)$. Note the two different color scales, both given in units of $D^{[|1\rangle\langle 1|]}(0)$, indicating the small difference between the two histograms.

both histograms, see Fig. 2(c), we already clearly observe the circular symmetric character of the single photon phase space distribution. The small deviation from an ideal circular symmetry is explained by a slight coherent admixture of the vacuum $|0\rangle$ to the single photon Fock state $|1\rangle$ due to small errors in the state preparation.

To further analyze the data we calculate the moments

$$\langle(\hat{S}^\dagger)^n \hat{S}^m\rangle_\rho = \int d^2S (S^*)^n S^m D^{[\rho]}(S) \tag{4}$$

of the two histograms up to a given order that is chosen to be $n + m = 4$ in our experiments. This specific choice is justified later in the text. When noise and signal are uncorrelated the calculated moments correspond to the operator averages

$$\langle(\hat{S}^\dagger)^n \hat{S}^m\rangle_\rho = G^{(n+m)/2} \sum_{i,j=0}^{n,m} \binom{m}{j}\binom{n}{i} \langle(a^\dagger)^i a^j\rangle \times \langle h^{n-i}(h^\dagger)^{m-j}\rangle, \tag{5}$$

reducing to $\langle(\hat{S}^\dagger)^n \hat{S}^m\rangle_{|0\rangle\langle 0|} = G^{(n+m)/2}\langle h^n (h^\dagger)^m\rangle$ when a is in the vacuum state. Equation (5) can then be inverted to calculate the moments $\langle(a^\dagger)^n a^m\rangle$ from $\langle(\hat{S}^\dagger)^n \hat{S}^m\rangle_\rho$ and $\langle(\hat{S}^\dagger)^n \hat{S}^m\rangle_{|0\rangle\langle 0|}$ up to the desired order, 4 in this case, as shown in Fig. 3(a). We note that the quadrature histograms are normalized such that the zeroth order moments are always unity for all prepared states. The off diagonal elements in the moment matrix express coherences between different photon number states. They vanish for states with circular symmetric phase space distributions such as pure Fock states or thermal states. For the Fock state $|1\rangle$ [Fig. 3(a)], we observe that all off diagonal moments are close to zero. In addition, we note that the fourth order moment $\langle(a^\dagger)^2 a^2\rangle$ is also close to 0, indicating antibunching of the prepared single photon states [9]. In contrast, a thermal state with the same mean photon number would display vanishing off diagonal moments but finite diagonal fourth order moments. Experimentally, for the single photon Fock state, the aforementioned residual coherent admixture of the vacuum state leads to a nonvanishing small mean amplitude $|\langle a\rangle| = 0.044$ and a slightly reduced mean photon number $\langle a^\dagger a\rangle = 0.91$. For an integration time of 12 h for each state, we find errors of the fourth order moments to be approximately ± 0.1 where the statistical error in the moments is known to increase exponentially with increasing order [8]. In comparison, the estimated statistical errors for the first, second, and third order moments are approximately 1.5×10^{-3}, 4.5×10^{-3}, and 1.5×10^{-2}, respectively. The errors have been estimated from the standard deviation of the moments acquired in repeated measurements of the distributions.

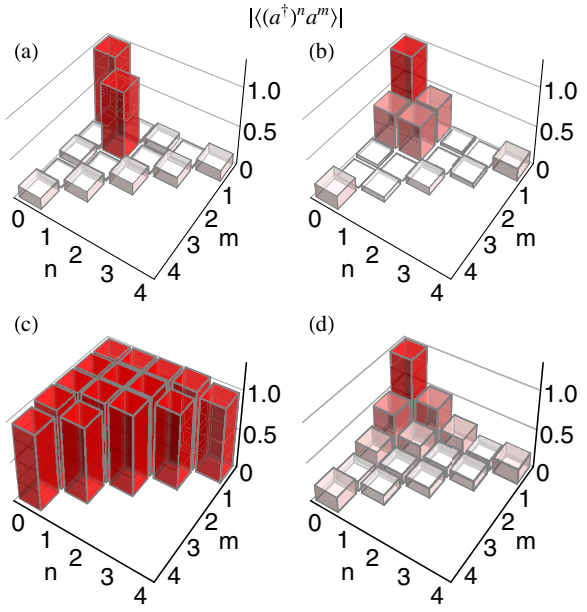

FIG. 3 (color online). Absolute value of the normally ordered moments $|\langle(a^\dagger)^n a^m\rangle|$ up to fourth order for (a) a single photon Fock state, (b) a superposition state $(|0\rangle - |1\rangle)/\sqrt{2}$, and two coherent states with amplitude (c) $\alpha = 1$ and (d) $\alpha = 0.5$.

We have also prepared and analyzed superposition states of the type $(|0\rangle + e^{i\phi}|1\rangle)/\sqrt{2}$; see Fig. 3(b). The relative phase ϕ is controlled by the phase of the corresponding qubit state that is mapped into the resonator. For this class of states, the mean amplitude ideally equals the mean photon number $|\langle a\rangle| = \langle a^\dagger a\rangle = 0.5$. The first equality remains approximately valid even if the state is slightly mixed with the vacuum. We have been able to use this property to determine the effective gain G of our amplifier chain because first and second order moments have a different characteristic scaling with G. This allowed us to scale X and P axes of the histograms (Fig. 2) such that they correspond to the real and imaginary part of $a + h^\dagger$. From our measurement data, we extract $|\langle a\rangle| = 0.466$, which is close to the expected value.

To further confirm the validity of our scheme, we have generated coherent states $|\alpha\rangle$ with amplitude $\alpha = 1$ and $\alpha = 0.5$ by applying 10 ns square coherent pulses with controlled amplitude to the weakly coupled input port of the resonator. The moments of coherent states are given by $\langle(a^\dagger)^n a^m\rangle = (\alpha^*)^n \alpha^m$. For $\alpha = 1$ all moments are observed to be close to 1 [Fig. 3(c)], as expected. This also demonstrates that systematic errors in the detection chain, such as small nonlinearities, are negligible since all moments take their expected values. For $\alpha = 0.5$ [Fig. 3(d)], the measured moments decay exponentially with $\langle(a^\dagger)^n a^m\rangle = 0.5^{n+m}$, as expected. The fourth order moments appear larger than the third order ones, due to their larger statistical error.

From the measured moments we have reconstructed the Wigner function $W(\alpha)$ for a single photon Fock state and its superposition with the vacuum (Fig. 4). It is sufficient to evaluate [1]

$$W(\alpha) = \sum_{n,m} \int d^2\lambda \frac{\langle(a^\dagger)^n a^m\rangle(-\lambda^*)^m \lambda^n}{\pi^2 n! m!} e^{(-1/2)|\lambda|^2 + \alpha\lambda^* - \alpha^*\lambda}$$

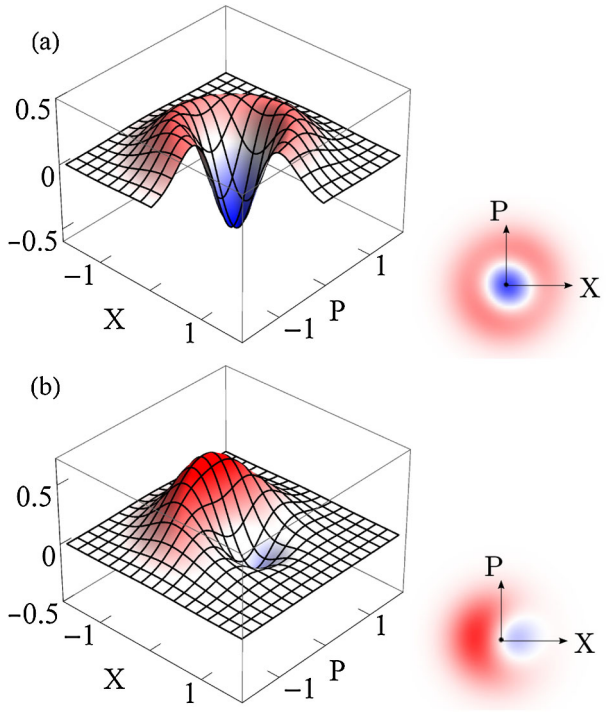

FIG. 4 (color online). Wigner function W $(\alpha = X + iP)$ for (a) a single photon Fock state and (b) a superposition state both reconstructed from the measured moments shown in Fig. 3.

up to order $n + m = 3$ because $\langle (a^\dagger)^2 a^2 \rangle \sim 0$. In general, all higher order moments with $n + m \geq 2N - 1$ have to be zero if one diagonal moment $\langle (a^\dagger)^N a^N \rangle$ vanishes, which follows from the fact that diagonal moments $\langle k|(a^\dagger)^n a^n|k\rangle$ with $n > k$ are zero for Fock states $|k\rangle$. The Wigner function of the single photon Fock state [Fig. 4(a)] shows clear negative values which indicate the quantum character of the observed state. The slight shift of $|\langle a \rangle| = 0.044$ from the phase space origin that we already observed in the raw measurement data [Fig. 2(c)] of the $|1\rangle$ state is also apparent in the reconstructed Wigner function. The superposition state $(|0\rangle - |1\rangle)/\sqrt{2}$ displayed in Fig. 4(b) has a finite mean amplitude which leads to the finite center of mass of the distribution. Still, negative values in the distribution persist, illustrating the quantum coherence between the $|0\rangle$ and $|1\rangle$ state. We have also varied the relative phase ϕ of the superposition states and have observed the expected rotation of the Wigner function (data not shown).

In summary, we have measured the moments of itinerant single microwave photons and small coherent fields up to fourth order using linear amplification, quadrature amplitude detection, and efficient data analysis. We have implemented a method to separate the quantum signal from the amplifier noise in a measurement setup with only one detection channel. We believe that propagating microwaves will be investigated more intensely in the context of future quantum optics and also quantum information processing experiments [27] where low noise parametric amplifiers [28–30] have the potential to significantly improve the detection efficiency.

The authors would like to acknowledge fruitful discussions with A. Blais, M. da Silva, G. Milburn, and B. Sanders. This work was supported by the European Research Council (ERC) through a Starting Grant and by ETHZ.

Note added in proof.—A different method was recently used to obtain a similar state reconstruction [31].

[1] S. Haroche and J.-M. Raimond, *Exploring the Quantum: Atoms, Cavities, and Photons* (Oxford University Press, Oxford, England, 2006).
[2] J.-M. Raimond, M. Brune, and S. Haroche, Rev. Mod. Phys. **73**, 565 (2001).
[3] A. Blais *et al.*, Phys. Rev. A **69**, 062320 (2004).
[4] A. Wallraff *et al.*, Nature (London) **431**, 162 (2004).
[5] M. Hofheinz *et al.*, Nature (London) **459**, 546 (2009).
[6] A. Houck *et al.*, Nature (London) **449**, 328 (2007).
[7] Y.-F. Chen *et al.*, arXiv:1011.4329v1.
[8] M. P. da Silva, D. Bozyigit, A. Wallraff, and A. Blais, Phys. Rev. A **82**, 043804 (2010).
[9] D. Bozyigit *et al.*, Nature Phys. **7**, 154 (2010).
[10] J. M. Chow *et al.*, Phys. Rev. A **82**, 040305 (2010).
[11] A. Palacios-Laloy *et al.*, Nature Phys. **6**, 442 (2010).
[12] O. Astafiev *et al.*, Science **327**, 840 (2010).
[13] C. Gerry and P. L. Knight, *Introductory Quantum Optics* (Cambridge University Press, Cambridge, England, 2005).
[14] H. J. Carmichael, *Statistical Methods in Quantum Optics 1* (Springer-Verlag, Berlin, 1999).
[15] V. Bužek, G. Adam, and G. Drobný, Phys. Rev. A **54**, 804 (1996).
[16] A. I. Lvovsky and M. G. Raymer, Rev. Mod. Phys. **81**, 299 (2009).
[17] D. T. Smithey, M. Beck, and M. G. Raymer, Phys. Rev. Lett. **70**, 1244 (1993).
[18] D. Welsch, W. Vogel, and T. Opatrný, arXiv:0907.1353v1.
[19] C. M. Caves, Phys. Rev. D **26**, 1817 (1982).
[20] A. A. Clerk *et al.*, Rev. Mod. Phys. **82**, 1155 (2010).
[21] E. P. Menzel *et al.*, Phys. Rev. Lett. **105**, 100401 (2010).
[22] M. Hofheinz *et al.*, Nature (London) **454**, 310 (2008).
[23] C. W. Gardiner and M. J. Collett, Phys. Rev. A **31**, 3761 (1985).
[24] D. Walls and G. Milburn, *Quantum Optics* (Springer-Verlag, Berlin, 1994).
[25] H. Nha, G. Milburn, and H. J. Carmichael, New J. Phys. **12**, 103010 (2010).
[26] M. S. Kim, Phys. Rev. A **56**, 3175 (1997).
[27] P. Kok *et al.*, Rev. Mod. Phys. **79**, 135 (2007).
[28] M. A. Castellanos-Beltran and K. W. Lehnert, Appl. Phys. Lett. **91**, 083509 (2007).
[29] N. Bergeal *et al.*, Nature (London) **465**, 64 (2010).
[30] T. Yamamoto *et al.*, Appl. Phys. Lett. **93**, 042510 (2008).
[31] F. Mallet, M. A. Castellanos-Beltran, H. S. Ku, S. Glancy, E. Knill, K. D. Irwin, G. C. Hilton, L. R. Vale, and K. W. Lehnert, Phys. Rev. Lett. **106**, 220502 (2011).